Seasonal variability of crustal and marine trace elements in the aerosol at Neumayer Station, Antarctica

ROLF WELLER*[1], JANINA WÖLTJEN[1,2]; CLAUDIA PIEL[1], ROSA RESENBERG[1], DIETMAR WAGENBACH[3], GERT KÖNIG-LANGLO[1] and MICHAEL KRIEWS[1], *[1]Alfred Wegener Institute for Polar and Marine Research, Am Handelshafen 12, 27570 Bremerhaven, Germany, [2]Present address: School of Environmental Sciences, University of East Anglia, Norwich NR4 7TJ, UK, [3]Institut für Umweltphysik, University Heidelberg, Im Neuenheimer Feld 229, D-69120 Heidelberg, Germany

* Correponding author.
e-mail: Rolf.Weller@awi.de

Version 30.04.2008

52

53   ABSTRACT

54   Atmospheric trace element concentrations were measured from March 1999 through De-

55   cember 2003 at the Air Chemistry Observatory of the German Antarctic station Neumayer by

56   inductively coupled plasma – quadrupol mass spectrometry (ICP-QMS) and ion chromatogra-

57   phy (IC). This continuous five year long record derived from weekly aerosol sampling re-

58   vealed a distinct seasonal summer maximum for elements linked with mineral dust entry (Al,

59   La, Ce, Nd) and a winter maximum for the mostly sea salt derived elements Li, Na, K, Mg,

60   Ca, and Sr. The relative seasonal amplitude was around 1.7 and 1.4 for mineral dust (La) and

61   sea salt aerosol (Na), respectively. On average a significant deviation regarding mean ocean

62   water composition was apparent for Li, Mg, and Sr which could hardly be explained by mir-

63   abilite precipitation on freshly formed sea ice. In addition we observed all over the year a not

64   clarified high variability of element ratios Li/Na, K/Na, Mg/Na, Ca/Na, and Sr/Na. We found

65   an intriguing co-variation of Se concentrations with biogenic sulfur aerosols (methane sul-

66   fonate and non-sea salt sulfate), indicating a dominant marine biogenic source for this element

67   linked with the marine biogenic sulfur source.

68

1. Introduction

69

70   The nearly completely ice covered Antarctic continent is virtually free of primary and sec-

71   ondary aerosol sources while the Southern Ocean is by far the dominant source to the Antarc-

72   tic aerosol body making atmospheric sea salt and biogenic sulfur the major aerosol compo-

73   nents (Wagenbach et al., 1998; Minikin et al., 1998). Terrestrial sources are limited to some

74   insular rocky regions (on the Antarctic peninsula, in the coastal dry valleys and on high

75   mountain ranges) and volcanic activity of Mt. Erebus. Nowadays, minor anthropogenic emis-

76   sions arising from fossil fuel combustion during research and tourism activities may be con-

77   sidered as well. On the whole these natural and anthropogenic sources constitute local or

78   regional trace element emissions of mineral dust, sulfur, and specific heavy metals which are

79   thought to be of minor importance for the overall aerosol budget of Antarctica. Therefore,

80   Antarctica offers an outstanding place to study the background composition and the natural

81   biogeochemical cycling of aerosol.

82   Apart from ion analyses, only limited trace element measurements have been conducted so

83   far in Antarctic aerosol samples as: at South Pole (Zoller et al., 1974; Cunningham and Zoller,

84   1981; Tuncel et al., 1989), at the Antarctic peninsula (Dick, 1991; Artaxo et al., 1992) and at

85   coastal areas (i.e. Neumayer Station, Görlach, (1988) and Wagenbach et al. (1988)). In recent

86   years the need for long term background aerosol studies, especially addressing the trace ele-

87   ment composition, has been recognized. Certain heavy metals (e.g. Pb, Cd, Cr) can be em-

88   ployed as valuable tracers for the growing impact of anthropogenic heavy metal emissions for

89   remote Antarctica (Wolff and Suttie, 1994; Wolff et al., 1999; Planchon et al., 2002). Fur-

90   thermore, mineral dust derived trace elements like Fe may act as micronutrients affecting the

91   biological activity of the ocean (Jickells et al., 2005), e.g. the atmospheric CO_2 burial (Bopp

92   et al., 2003; Wolff et al., 2006) and the emission of dimethyl sulfide (DMS) (Turner et al.,

93   2004), which is globally the most important precursor for natural sulfate aerosol. Finally,

Version 30.04.2008

94   mineral dust and sea salt profiles retrieved from polar ice cores have proven to provide a

95   wealth of paleoclimatic information (e.g. Petit et al., 1999; Wolff et al., 2006; Fischer et al.,

96   2007; Ruth et al., 2007). For improving the interpretation of these records, a better knowledge

97   about long range transported continental dust and regional derived sea salt would be needed,

98   especially including the seasonality of their atmospheric loading and entry into the Antarctic

99   continent. Concerning sea salt aerosol, the formation on freshly formed sea ice, associated

100   with a significant sea salt fractionation, has been put forward as an alternative source (Rankin

101   et al., 2000 and 2002; Wolff et al., 2003) to the accepted process by wind induced bubble

102   bursting over open ocean water (Monahan et al., 1986). If the significance of this source

103   proves true, it would entail a paradigm shift in the interpretation of sea salt profiles from polar

104   ice cores (Wolff et al., 2003).

105   Here, we present atmospheric trace element records mainly associated with mineral dust

106   and marine sources which are continuously observed between 1999-2003 at the German

107   Antarctic Neumayer Station. Primarily focusing on seasonal aspects, the weekly filter samples

108   were analysed by ICP-QMS for the trace element Li, Na, K, Mg, Ca, Sr, Al, La, Ce, Nd, and

109   Se. The ICP-QMS results are supported by our regular IC analyses providing complementary

110   information on the ionic aerosol composition with respect to methane sulfonate, sulfate, Na^+,

111   NH_4^+, K^+, Mg^{2+}, and Ca^{2+}.

112

113   **2. Methods**

114   **2.1. Measurement Site and Meteorological Conditions**

115   Aerosol sampling was made at the Air Chemistry Observatory, about 1.5 km south of Neu-

116   mayer station (70° 39' S, 8° 15'W). During the summer months, the bay and the nearby ice

117   edge are mainly free of sea ice and there is always open water present. Apart from a few

118   nunataks about 100 km south of the station there are no ice-free land surfaces near Neumayer,

Version 30.04.2008

119   and the probability of contact with air masses from ice-free continents is small. In general

120   there are two different wind regimes: (1) Strong synoptically affected winds are from the East

121   with infrequent geostrophically intensified switches to the West and (2) weak katabatic winds

122   from southern directions. The air mass transport pattern to Neumayer Station was investigated

123   by Kottmeier and Fay (1998) and a more detailed picture on the climatology at Neumayer

124   Station can be found in König-Langlo et al. (1998).

125   Aerosol was collected on Whatman 541 cellulose filters which were precleaned by soaking

126   in HCl followed by rinsing with de-ionize water until virtually no enhancement of the electro-

127   lytical conductivity could be detected. The aerosol was continuously sampled at 120 m^3 h^{-1}

128   by two filters (diameter 240 mm) in series using a ventilated electropolished stainless steel

129   inlet stack (total height about 8 m above the snow surface) with a 50% aerodynamic cut-off

130   diameter around 7-10 µm at wind velocities between 4-10 m s^{-1}. This high volume sampling

131   technique is part of the continuous long-term observation programme carried out since 1983

132   at Neumayer. Here we refer to samples taken from March 1999 through December 2003.

133   These data were based on a sampling period of typically 7 days which corresponds to a probe

134   volume of around 2_x10^4 m^3 STP. A more detailed description of the sampling procedure itself

135   is given in Wagenbach et al. (1988).

136   Local pollution by vehicles and the base itself is a potential problem for many measure-

137   ments concerning the background status of the Antarctic troposphere. To ensure contamina-

138   tion free air sampling, the Air Chemistry Observatory is situated in a clean air facility ap-

139   proximately 1.5 km south of Neumayer. Due to the fact that northerly wind directions are

140   very rare, contamination from the base can be excluded for most of the time. Additionally, the

141   power supply (20 kW) is provided by cable from the main station, thus no fuel driven genera-

142   tor is operated in the observatory vicinity. Finally, contamination-free sampling is controlled

143   by the permanently recorded wind velocity, wind direction and by the condensation particle

Version 30.04.2008

144   (CP) concentration. Contamination was indicated for each of the following criteria: Wind

145   direction within a 330°-30° sector, wind velocity <2.0 m s^{-1} and/or CP concentrations (meas-

146   ured by a TSI CPC 3022A particle counter) >2500 cm^{-3} during summer, >800 cm^{-3} during

147   spring/autumn and >400 cm^{-3} during winter. The CP threshold values were chosen based on

148   our more than 20-year long CP record from Neumayer, demonstrating that CP concentrations

149   above the corresponding levels can usually be traced back to local pollution. In case of con-

150   tamination, given by these criteria, an automatic interrupt of the sampling procedure was

151   initiated within one second (shut down of the pumps and closing the electromotive valves

152   typically needed around 10 seconds). Sampling was restarted after recurrence of clean air

153   conditions and a delay of two minutes. However, most of the data loss was provoked by

154   blizzards and drifting snow (wind velocity >20 m s^{-1}). During such harsh weather conditions

155   aerosol sampling has to be switched off (due to the danger of snow entering the inlet) which

156   entailed a downtime of roughly 10% of the observation period. Note, that <2% of data loss

157   was actually caused by potential contamination.

158

159   **2.2. Analytical Methods**

160   **2.2.1. ICP-QMS Analysis**

161   Trace element analysis was performed by means of ICP-QMS (ELAN 6000, Sciex/Perkin

162   Elmer) equipped with a cross-flow nebulizer as sample introduction system. The alignment of

163   the instrument (plasma torch, ion lens, gas flow, nebulizer) was checked and adjusted before

164   analysis by daily performance solutions containing a mixture of 10 ng g^{-1} Mg, Ba, Ce, Pb, and

165   Rh. One half of each filter was used for trace element analysis, while another 1/6 of each filter

166   was used for IC analysis (see below). For trace element analyses we chose a total digestion of

167   the samples in order to quantitatively dissolve all mineral compounds, which is not been

168   given by simple acidic (HNO$_3$) leaching (Lindberg and Harris, 1983; Reinhardt et al., 2003,

169 Table 5 therein). Thus these aliquots were subject to a pressurized digestion system (DAS

170 100, Picotrace) at 200°C in a mixture containing HNO_3 (suprapure, 65%, Merck, sub-boiling

171 bi-distilled), HF (suprapure, 40%, Merck, sub-boiling bi-distilled) and H_2O_2 (suprapure, 30%,

172 Merck). With this device a series of 24 samples could be digested in parallel. Each series

173 included one filter blank and a certified reference sample (NIST 1648 urban particulate mat-

174 ter). For calibration we used commercially available standard solutions (10^4 ppb multielement

175 verification standard 1 and 2, Perkin Elmer) which were generally applied in 1 ppb, 10 ppb,

176 and 100 ppb concentrations (1 ppb corresponds to 1 ng of each element in 1 g solute). Each

177 sample was spiked by 10 ppb Rh as internal standard to normalize the signal intensities and

178 compensate instrumental sensitivity variations. The instrumental detection limits (IDL) were

179 derived from 60 blank solutions and correspond to three times the standard deviation (std) of

180 these blank values (Table 1). Based on the results of the NIST reference material, the retrieval

181 for each element to be discussed here was generally between 95% and 100%. When analysing

182 the filter samples of the years 2002 and 2003 we were frequently faced with abnormally

183 elevated Al-blanks prohibiting further evaluation. Thus the time series of this period appeared

184 fragmentary. Due to these unexplained analytical problem, we decided to use the consistently

185 measured La as mineral dust tracer and reference element for calculating crustal enrichment

186 factors.

187   The variability of the filter procedure blanks clearly governed the overall accuracy as well

188 as the analytical detection limits. These estimates were derived from the variation of 49 iden-

189 tically processed procedure blanks and include possible contributions by the previously

190 cleaned filters and any effects arising from handling and storage. We conservatively estimated

191 the method detection limits (MDL) as three times the standard deviation (std) of these overall

192 blank values (Table 1). In addition to this blank induced uncertainty, relative ICP-QMS cali-

193 bration errors were considered. In short, the combined uncertainty was found to be approxi-

194　　mately between ±8% and ±12% for element concentrations above three times the correspond-

195　　ing MDL. It increased from around ±(15-20)% approaching 3xMDL level to roughly (+50/-

196　　100)% close to the MDL. The final atmospheric concentrations (in ng m^{-3} or pg m^{-3}) were

197　　calculated from the blank corrected element amounts and the corrected sampled air volume to

198　　standard conditions (273.16 K and 1013 hPa).

199

200　　**2.2.2. IC Analysis**

201　　　　The extraction of the aliquots for IC analysis included soaking and shaking in 50 ml MilliQ

202　　water, followed by ultrasonic treatment for 15 minutes. All samples were analyzed for meth-

203　　ane sulfonate (MS), Cl^-, Br^-, NO_3^-, SO_4^{2-}, Na^+, NH_4^+, K^+, Mg^{2+}, and Ca^{2+} by IC analysis. For

204　　details concerning IC set up, the determination of accuracy and detection limits see Piel

205　　(2004). Errors were determined from the blank variability, the typical IC error (calibration

206　　error and baseline noise), and the error from the sample air volume. In short, the combined

207　　uncertainty was between ±5% and ±11% for the components MS, Cl^-, NO_3^-, SO_4^{2-}, Na^+, K^+,

208　　Mg^{2+}, and Ca^{2+} and approximately ±27% for species Br^- and NH_4^+. Non-sea salt sulfate (nss-

209　　SO_4^{2-}) concentrations were calculated by subtracting the concentration of the sea salt derived

210　　sulfate from the total SO_4^{2-} concentration (in ng g^{-1}). We used Na^+ as sea salt reference spe-

211　　cies and the sulfate to sodium ratio in bulk sea water of 0.252 for November to February, and

212　　due to the potential impact of sea salt fractionation by frost flower formation a factor of 0.07

213　　for winter (March – October) samples (Wagenbach et al., 1998). Note that with our sampling

214　　technique, gaseous HCl, HBr, HNO_3, and NH_3 were partly collected on the filter material and

215　　contributed to the reported Cl^-, Br^-, NO_3^-, and NH_4^+ concentrations.

216　　　　For the elements Na, K, Mg, and Ca an inter-comparison with the corresponding concentra-

217　　tions measured by IC was possible. A reduced major axis regression (RMA) revealed a good

218　　agreement between ICP-QMS and IC for Na and Mg, while the ICP-QMS systematically

Version 30.04.2008

219   provided higher K and lower Ca concentrations (Table 2). For these two elements the results

220   from the IC-analytics were used throughout the paper because they appeared more reliable.

221   Apart from known problems associated with the detection of K and Ca by ICP-QMS (mainly

222   interferences from Ar carrier gas of the plasma), a possible explanation in case of Ca may be

223   the formation of hardly soluble CaF_2 during digestion. The relatively high scatter of the data

224   around the regression line, expressed by somewhat low regression coefficients r^2 (Table 2),

225   may partly be due to the fact that ICP-QMS and IC analyses were performed with different

226   aliquots of the corresponding filters.

227

228

229   ## 3. Results and Discussion

230   ### 3.1. Classification of Trace Elements

231   We first calculated for each element M the so-called crustal EF_{crust} and sea salt EF_{ss} enrich-

232   ment factors, respectively as:

233
$$EF_{crust} = \frac{(M/La)_{aerosol}}{(M/La)_{crust}}, \qquad EF_{ss} = \frac{(M/Na)_{aerosol}}{(M/Na)_{ss}}$$

234   For reasons discussed in the analytical section, we chose as marker for mineral dust La and

235   refer to the crustal composition reported in Wedepohl (1995). Note that at Neumayer Ca is

236   largely sea salt derived (see below) and thus an unfavourable tracer for mineral dust. For the

237   corresponding EF_{ss} we rely on standard mean ocean composition reported in Holland (1993).

238   In Fig. 1 the results are presented for winter and summer. Because the ocean is well mixed,

239   even small deviations from the standard mean ocean composition indicate that either the

240   given component was only partially associated with sea salt or a sea salt fractionation during

241   aerosol formation/transport occurred. The situation is intrinsically much more complicated in

242   case of mineral dust. First of all the crustal composition of the earth exhibits a pronounced

Version 30.04.2008

243   variability (Wedepohl, 1995). Apart from this, weathering and mineral dust generating proc-

244   esses usually entail a distinct fractionation. Also the crustal element composition may signifi-

245   cantly differ between mean crust, soil and the small (clay) particles being readily long range

246   transported. Here, we conservatively assume that EF_{crust} values above 10 point at a negligible

247   mineral dust source. The enrichment factors indicate crustal material as the main source for

248   the elements Al, Nd, and Ce, while, on the other hand, Li, K, Mg, Ca, and Sr were primarily

249   sea salt derived elements, though this dissection appears equivocal for Li. Selenium in con-

250   trast was found to be highly enriched relative to crust, but also with respect to (sea salt) Na

251   pointing to anthropogenic or biogenic sources.

252

253   **3.2. Overview on the Trace Element Concentrations measured at Neumayer Station**

254   Table 3 gives a compendium of the trace element concentrations measured five years at

255   Neumayer Station. In addition individual time series of trace elements representative for sea

256   salt aerosol (Li, Na, Sr) and mineral dust (Al, La, Ce, Nd) species are presented in Figures 2

257   and 3. Generally, trace element concentrations at Neumayer exhibited a striking inter-annual

258   and seasonal variability. Apart from the general sparseness of data available from other Ant-

259   arctic sites, the intrinsic strong variability makes a coherent assessment of the inter-site differ-

260   ences a difficult task. Especially the extraordinarily high atmospheric Se and Al levels re-

261   ported by Artaxo et al. (1992) remain unexplained (Table 4).

262   Görlach (1988) used acid extractable Mn and Wagenbach (1996) combined Mn and Al as

263   mineral dust proxy at Neumayer. Converting the reported Mn from Görlach (1988) into corre-

264   sponding La concentrations (using a mean crust composition given in Wedepohl (1995), i.e.

265   Mn/La = 23.9) resulted in a summer maximum of around 1.1 pg m^{-3} and a winter minimum of

266   0.21 pg m^{-3}. This is systematically lower (by 0.21 pg m^{-3} and 0.35 pg m^{-3}, respectively) but

267   still in fair agreement with our La results (Table 3). A pronounced seasonal Al (i.e. mineral

Version 30.04.2008

268 dust) maximum during austral summer was evident at all sites, with a mineral dust entry

269 tentatively higher at coastal Neumayer compared to continental South Pole (Table 4). The

270 data from the Antarctic Peninsula tip appeared contradicting, and the mentioned outstanding

271 high Al values reported by Artaxo et al. (1992) might most probably be caused by sporadic

272 local dust production from the rocky adjacencies. In contrast to the observed marginal gradi-

273 ent from coastal to continental Antarctica for mineral dust related trace elements, Na (i.e. sea

274 salt) concentrations were about an order of magnitude higher at coastal sites.

275

276 **3.3. Seasonal Aspects**

277 **3.3.1. Synopsis of the seasonality of the aerosol budget at Neumayer**

278 In order to assess the relative composition of the aerosol (by mass) and its seasonality, we

279 included the relevant ionic compounds. Therefore we considered the aerosol compounds sea

280 salt (calculated from the measured Na) mineral dust (calculated from the measured La) and

281 further MS, $nss\text{-}SO_4^{2-}$, Cl^-, NO_3^-, and NH_4^+ from the IC analyses. Clearly, the aerosol at Neu-

282 mayer was dominated by sea salt particles (Fig. 4), even during summer when biogenic sulfur

283 emissions reach their distinct annual maximum (Minikin et al., 1998), while mineral dust was

284 generally a minor compound with a maximum mass fraction of about 5% during summer.

285 Figure 5 shows in more detail the annual cycle of the compounds sea salt, mineral dust and

286 biogenic sulfur (sum of MS and $nss\text{-}SO_4^{2-}$). In terms of aerosol composition (biogenic, sea

287 salt, and mineral dust) the polar winter seemed confined between April and end October with

288 the turn of the seasons occurring in March/April and October/November.

289

290 **3.3.2. Seasonality of mineral dust and sea salt entry at Neumayer**

291 Figures 2 and 3 indicate that mineral dust and sea salt derived trace elements (Al, La, Ce,

292 Nd, and Li, Na, K, Mg, Ca, Sr, respectively) were characterized by distinct mean annual

293   cycles. In Figure 6 the mean seasonal cycle of the crustal and sea salt reference are displayed

294   in monthly concentrations (± standard deviation). The seasonality was most pronounced for

295   the crustal elements with a distinct concentration maximum from October through March,

296   while for sea salt aerosol a broad maximum between April and September was evident. The

297   mean relative seasonal amplitude, i.e. the mean maximum normalized to the corresponding

298   annual mean, was around 1.7 and 1.4 for mineral dust (La) and sea salt aerosol (Na), respec-

299   tively. In addition, enrichment factors also exhibited a distinct seasonality, with higher EF_{crust}

300   but lower EF_{ss} in winter and vice versa (Figure 1). A possible reason for this finding might be

301   the seasonality of dust and sea salt entry observed at Neumayer. During the seasonal maxi-

302   mum of atmospheric dust entry in summer and sea salt concentrations in winter, the corre-

303   sponding enrichment factors were lowest due to the dilution of a given enrichment effect by

304   enhanced crustal dust or sea salt material, repectively.

305   The observed seasonality for mineral dust appeared consistent with previous studies from

306   Neumayer (Görlach, 1988; Wagenbach et al., 1988, Wagenbach, 1996), as well as South Pole

307   (Cunningham and Zoller, 1981; Tuncel et al., 1989), where Mn and Al was used as tracer for

308   mineral dust, respectively. A thorough evaluation of sea salt aerosol concentrations measured

309   at various coastal stations was given in Wagenbach et al. (1998). In agreement with our find-

310   ings, these authors reported a broad Na maximum during winter at Neumayer, which has also

311   been observed at South Pole (Tuncel et al., 1989). In general, an annual cycle of aerosol

312   components observed at remote, source free sites can be attributed to a combination in the

313   seasonality of the source strength and atmospheric transport processes. While for sea salt

314   aerosol regional or even local sources have to be considered, the source regions for mineral

315   dust on the surrounding continents are more than 4000 km away and consequently long range

316   transport, most probably via the free troposphere, is decisive (Genthon, 1992; Krinner and

317   Genthon, 2003). It is believed that the main provenances for Antarctic mineral dust are the

318   Patagonian loess regions (Smith et al., 2003). The seasonal contrast of Patagonian dust fluxes

319   seems by far not as distinct as those of the atmospheric rare earth element (equivalent to

320   mineral dust) concentrations at Neumayer, though a broad maximum between October and

321   March is discernible (Gaiero et al., 2003, Figure 14 therein). In addition to this somewhat

322   ambiguous source strength seasonality, we may expect a clear annual cycle in the atmospheric

323   mixing height above continents (typically maximum during summer). Since long range dust

324   transport to Antarctica is favoured via the mid troposphere, a more effective transfer of dusty

325   boundary layer into high altitudes during the summer half year would be consistent with a

326   Neumayer summer maximum as well. This explanation is supported by measurements of a

327   basically similar seasonality seen at this site for the long lived ^{222}Rn decay product ^{210}Pb

328   (Wagenbach et al., 1988), known to have a rather constant (continental) emission rate and to

329   be less effectively washed out than the typically coarse mode mineral dust particles. Therefore

330   the observed mineral dust maximum at Neumayer is probably a combined result of the sea-

331   sonality in dust generation and the more efficient uplift of dust loaded air into the free tropo-

332   sphere in summer.

333   The most efficient global mechanism producing sea salt aerosol is bubble bursting during

334   whitecap formation and dispersion of wave crests by surface winds over open ocean waters

335   (Monahan et al., 1986). Thus, sea salt production exhibits a strong dependency on wind speed

336   (Fitzgerald, 1991). Compatible with this perception is the fact that storminess and wind veloc-

337   ity exhibit a broad maximum during the winter months at Neumayer (Fig. 7). However, as for

338   the individual data points there was virtually no correlation between wind velocity and ob-

339   served Na concentrations ($r^2 = 0.07$). Note that this was also true for our low volume aerosol

340   samples taken at daily resolution between October 2003 and February 2007 (teflon-nylon

341   filter combinations, analysed by IC). It seems that the general weather situation over the

342   South Atlantic was decisive and the most efficient sea salt production occurred during passing

Version 30.04.2008

343   cyclones (Wyputta, 1997). However, the sea salt aerosol loading at Neumayer should also

344   depend on the efficiency of the transport process, removal by wet deposition, and the actual

345   sea-ice cover. The interplay of these factors may have blurred a simple correlation with the

346   local wind speed. In this regard, however, we have to bear in mind that particles above an

347   aerodynamic diameter of around 7-10 µm, which may constitute a significant if not dominant

348   fraction of the sea salt aerosol mass from nearby sources, were not adequately sampled due to

349   the cut-off of our air inlet.

350   The formation of sea salt aerosols by frost flowers and associated processes suggested by

351   Wolff et al. (2003) should be most active between March and September, consistent with the

352   observed Na seasonality. Again it can be assumed that high wind velocities are still necessary

353   to finally create sea salt aerosols by dispersion and mobilisation of frost flowers, a process

354   which is actually not yet clarified.

355

356   **3.3.4. Sea salt fractionation**

357   There is some evidence that during wind induced sea salt aerosol generation over open

358   ocean waters, a fractionation of major ions (Na^+, Mg^{2+}, K^+, Cl^-, and SO_4^{2-}) relative to bulk

359   seawater is negligible, except for Ca^{2+} which appeared significantly enriched (Keene et al.,

360   2007). On the other hand, sea ice formation entails considerable sea salt fractionation which

361   could influence sea salt aerosol composition if freshly formed sea ice acts as a significant

362   source. Below -6.3°C solid $Na_2SO_4 \cdot 10H_2O$ (mirabilite) crystallizes, followed by $CaSO_4 \cdot 2H_2O$

363   (gypsum), and $NaCl \cdot 2H_2O$ (hydrohalite) precipitation at -22.2°C and -22.9°C, respectively

364   (Marion and Farren, 1999). A complete mirabilite precipitation, probably the dominant frac-

365   tionation process on freshly formed sea ice, would lead to a Na depletion of about 11.8% by

366   mass. Assuming simply that no fractionation would occur for the sea salt compounds Li, K,

367   Mg, and Sr, a corresponding increase of the enrichment factors EF_{ss} to around 1.12 should be

Version 30.04.2008

368   expected in sea salt aerosol for this species during winter when sea salt fractionation is most

369   probable. In fact, Rankin et al. (2000) found Mg and Ca enrichment factors in frost flower

370   samples near Halley Station ($EF_{ss}(Mg) = 1.16$, and $EF_{ss}(Ca) = 1.15$), roughly compatible with

371   mirabilite precipitation but indicating, if at all, a negligible gypsum precipitation. Also analy-

372   ses of individual aerosol particles sampled at the coastal Syowa Station evidenced fraction-

373   ated Mg-rich (and Ca-rich) sea salt particles (Hara et al., 2005).

374   Combining our ICP-QMS and IC results allows to determine sea salt fractionation for an

375   extended number of sea-salt related trace elements. In our approach we first corrected Li, K,

376   Mg, Ca, and Sr concentrations for the minor crustal contribution (which were generally be-

377   tween 1% and 8%) to derive enrichment factors $EF_{ss}(ssM)$ exclusively for the sea salt portion

378   of these elements. To be consistent, we generally referred ssK and ssCa values to ssNa all

379   taken from IC analyses, while for the other elements (Li, Mg, Sr) we relied on the ICP-QMS

380   results and related them to ssNa also determined by ICP-QMS. In this way we circumvent

381   potential discrepancies caused by systematic analytical differences of both methods (see

382   section 2.2.2).

383   All Na_{ss} based $EF_{ss}(ssM)$ values were strikingly variable throughout the year and, except

384   Ca, did not exhibit a significant seasonality as would have to be expected from a depleted

385   ssNa reference during winter (Figure 8). It is important to note that in terms of analytical

386   accuracy departures beyond ±20% (in the worst case, at very low concentrations, beyond

387   ±50%) from standard mean ocean water (SMOW) should be regarded as significant. Another,

388   but hardly conceivable reason for the scatter of $EF_{ss}(ssM)$ could be more than an order of

389   magnitude higher crustal M/La ratios (M = Li, Na, K, Mg, Ca, Sr) than reported by Wedepohl

390   (1995), which would strongly increase the crustal corrections and thus the uncertainty of the

391   calculated ratios. Concerning the medium departures of $EF_{ss}(ssM)$ from SMOW, Figure 8

392   reveals that ssLi and ssMg were enriched by a factor 2.2 and 1.2, respectively, while ssSr was

Version 30.04.2008

393   depleted throughout (EF_{ss}(ssSr) = 0.72). For ssK and ssCa the (median) deviation from

394   SMOW was not significant, except for the winter values of ssCa (EF_{ss}(ssCa)$_{winter}$ = 1.34). In

395   double-logarithmic plots of ssM (M = Li, K, Mg, Ca, Sr) versus the ssNa reference it becomes

396   apparent that departures from SMOW occurred equally over the whole measured concentra-

397   tion range and that for ssLi, ssMg, and ssSr the data points were displaced from the SMOW-

398   line (Fig. 9). Obviously, the high variability of EF_{ss}(ssM) in general, as well as the median

399   departures from SMOW for ssLi and ssSr cannot be explained by mirabilite precipitation

400   alone. Finally the scatter of the enrichment factors (Figures 8 and 9) were strikingly higher

401   than the results from recent laboratory investigations on sea salt aerosol formation over a

402   realistic air/sea interface (Keene et al., 2007). In summary, our results suggest that in the

403   present case additional unknown fractionation processes occurred during sea salt aerosol

404   production over the whole year at the interface air/sea or air/sea-ice or subsequently during

405   atmospheric transport and sampling.

406

407   **3.3.4. Source and seasonality of atmospheric Se**

408   It is believed that natural sources like sea spray, volcanoes, and the biosphere dominate the

409   global budget of atmospheric Se by around 60%, while the remaining anthropogenic sources

410   (basically fossil fuel combustion and mining) are mainly concentrated in the northern hemi-

411   sphere (Mosher and Duce, 1987). As noted by Mosher (1986), the natural and anthropogenic

412   Se cycles are closely linked through the biosphere. The distinct seasonal Se concentration

413   maximum during summer observed at Neumayer suggests a potential biogenic source.

414   Amouroux et al., (2001) have demonstrated that the production of gaseous selenium species

415   coincided with phytoplankton blooms responsible for dimethyl sulfide (DMS) emission. It

416   was found, that the sulfur atom in DMS can be substituted by selenium (Mosher et al., 1987;

417   Amouroux et al., 2001). Consequently, atmospheric Se should be closely coupled to the DMS

418   turnover. In fact we observed a significant correlation between Se and the end products of

419   photochemical DMS oxidation, MS and nss-SO_4^{2-} (r(MS) = 0.66; r(nss-SO_4^{2-}) = 0.67). The

420   co-variation of Se and MS time series is shown in Fig. 10. Even the inter-annual variability

421   largely coincided. Atmospheric Se concentrations found at South Pole were significantly

422   lower (Table 4) but showed the same seasonality with maximum values of 8.4±1.6 pg m^{-3}

423   during summer (winter concentration: 4.8±0.8 pg m^{-3} (Tuncel et al., 1989)), in accordance

424   with a prominent marine biogenic source which should be less discernible in continental

425   Antarctica.

426   Apart from this overall consistent picture there remain several open questions. First of all,

427   we have to consider that the sampling efficiency of total Se is not well specified. Inspecting

428   some of our Whatman 541 back-up filter showed no Se concentrations above the typical blank

429   value, in agreement with results by Mosher et al. (1987) who used Whatman 41 filters. In

430   contrast, Mosher (1986) reported on low sampling efficiencies (65%-45%) for this filter type

431   in his thesis. Apart from this, knowledge on speciation of atmospheric Se is poor. Apparently,

432   DMSe, elemental Se, as well as SeO_2 can be chemically transformed into water soluble se-

433   lenite (SeO_3^{2-}) and selenate (SeO_4^{2-}) in the atmosphere (Wen and Carignan, 2007). In marine

434   environments an enrichment of Se-compounds in sub-micron aerosol particles (mainly sea

435   salt particles) was suggested (Wen and Carignan, 2007). It is not clarified to what extend

436   volatile organic and inorganic Se species (e.g. DMSe, Se, SeO_2) are retained and likely

437   chemically transformed on the used filter material during the typical sampling interval of 7

438   days. Another issue are considerable Se background concentrations measured during polar

439   night (at Neumayer and South Pole) when regional biogenic activity ceases. This is in contrast

440   to negligible MS concentrations generally observed during winter (Figure 10). Hence we

441   tentatively assign wintertime atmospheric Se levels at Neumayer mainly to the global back-

442   ground load of Se. According to Cunningham and Zoller (1981), the atmospheric load of

Version 30.04.2008

443 volatile elements like As and Se at South Pole could also be influenced by volcanic emissions.

444 These authors ascribed a distinct Se peak in their time series to the explosive eruption of

445 Ngauruhoe volcano in New Zealand that happened in 1975. In our case, however, the contri-

446 bution of volcanic Se emissions should be, if at all, of minor importance due to the distance of

447 the sole presently active but calm volcanoes Mt. Erebus and Mt. Melbourne. Above all, the

448 observed seasonality of the Se signal at Neumayer can hardly be explained by volcanic impact

449 but might partly be responsible for background Se concentrations. Interestingly, wintertime

450 Se levels at Neumayer were about a factor of three higher compared to South Pole, where the

451 impact of Mt. Erebus should be more pronounced. For mineral dust derived trace elements

452 (Al, La) a similar but weaker gradient is apparent (Table 4), suggesting that the more pro-

453 nounced and deeper stable inversion layer at South Pole hampers down mixing of long range

454 transported trace compounds. In addition further minor, yet unexplained Se sources (local

455 contamination, still active regional biogenic emissions) possibly have to be considered at

456 Neumayer.

457

458

459 **5. Conclusion**

460 In contrast to the ionic composition of Antarctic aerosol, corresponding continuous long

461 term observations of atmospheric trace element concentrations are so far restricted to South

462 Pole and Neumayer. Even from these sites, complete year round data records do not cover

463 more than 5 years in series. Our results revealed a distinct and contrary seasonality of mineral

464 dust and sea salt load at Neumayer which, along with previous results, seems to be valid for

465 coastal as well as continental Antarctica. At coastal sites, mineral dust load appeared some-

466 what more pronounced. More observations from different sites are necessary to establish a

467 potential difference between continental and coastal Antarctica in trace element entry. Pro-

Version 30.04.2008

468   vided that mineral dust is widely uniformly distributed in the free troposphere above Antarc-

469   tica, this could give us some information on the role of the stable inversion layer, which is

470   most pronounced in continental Antarctica, as a barrier against air mass down mixing. This

471   would be especially interesting to scrutinize and constrain models addressing aerosol deposi-

472   tion in Antarctica. Another interesting point was the striking variability of the measured

473   ssM/ssNa ratios for M = Li, K, Mg, Ca, and Sr, suggesting that apart from sea salt formation

474   in sea ice covered regions itself, sea salt aerosol fractionation processes are not sufficiently

475   clarified. As a consequence we are still lacking a tracer to reliably assess sea salt production

476   on sea ice, a crucial point for the interpretation of sea salt records in polar ice cores. Marine

477   biochemistry was most probably the dominant source for Se. An interesting open question is,

478   how much Se is persistently deposited in polar snow and may serve as a proxy for biogenic

479   activity in polar ice cores. Clearly, more investigations on the atmospheric photochemistry of

480   marine biogenic selenium as well as the chemical nature of particulate atmospheric Se are

481   required.

482

483

Version 30.04.2008

References

488   Amouroux, D., Liss, P.S., Tessier, E., Hamren-Larsson, M., and Donard, O.F.X. 2001. Role

490   of oceans as biogenic sources of selenium. *Earth Planet. Sci. Lett.* **189**, 277-283.

491   Artaxo, P., Rabello, M.L.C., Maenhaut, W., and van Grieken, R. 1992. Trace elements and

492   individual particle analyis of atmospheric aerosols from the Antrctic peninsula. *Tellus* **44B**,

493   318-334.

494   Bopp, L., Kohfeld, K.E., Le Quéré, C., Aumont, O. 2003. Dust impact on marine biota and

495   atmospheric CO_2 during glacial periods. *Paleoceanography* **18**(2),

496   doi:10.1029/2002PA000810.

497   Cunningham, W.C. and Zoller, W.H. 1981. The chemical composition of remote area aero-

498   sols. *J. Aerosol Sci.,* **12**(4), 367-384.

499   Dick, A.L. 1991. Concentrations and sources of metals in the Antarctic Peninsula aerosol.

500   *Geochim. Cosmochim. Acta,* **55**, 1827-1836.

501   Fischer, H., Siggaard-Andersen, M.-L., Ruth, U., Röthlisberger, R., and Wolff, E. 2007.

502   Glacial/interglacial changes in mineral dust and sea-salt records in polar ice cores: sources,

503   transport, and deposition. *Rev. Geophys.* **45**, RG1002, doi:10.1029/2005RG000192.

504   Fitzgerald, J.W. 1991. Marine aerosols: A review. *Atmos. Environ. Part A,* **25**, 533-546.

505   Gaiero, D.M., Probst, J.-L., Depetris, P.J., Bidart, S.M., and Leleyter, L. 2003. Iron and other

506   metals in Patagonian riverborne and windborne materials: Geochemical control and trans-

507   port to the southern South Atlantic Ocean. *Geochim. Cosmochim. Acta* **67**(19), 3603-3623.

508   Genthon, C. 1992. Simulations of desert dust and sea-salt aerosol in Antarctica with a general

509   circulation model of the atmosphere. *Tellus* **44B**, 371-389.

510 Görlach, U. 1988. Die jahreszeitliche Variation von atmosphärischem Blei, Zink und Mangan

511   im antarktischen Küstenbereich, PhD-Thesis. Ruprecht-Karls-Universität Heidelberg, Hei-

512   delberg.

513 Hara, K., Osada, K., Kido, M., Matsunaga, K., Iwasaka, Y., Hashida, G., and Yamanouchi, T.

514   2005. Variations of constituents of individual sea-salt particles at Syowa station, Antarc-

515   tica. *Tellus* **57B**, 230-246.

516 Holland, H.D. 1993. The chemistry of atmosphere and oceans, John Wiley & Sons, 1. edition,

517   New York, 154-157.

518 Jickells, T.D., An, Z.S., Andersen, K.K., Baker, A.R., Bergametti, G., and co-authors. 2005.

519   Global Iron Connections Between Desert Dust, Ocean Biogeochemistry, and Climate. *Sci-*

520   *ence* **308**, 67-71, doi:10.1126/science.1105959.

521 Keene, W.C., Maring, H., Maben, J., Kieber, D.J., Pszenny, A.A.P. and co-authors. 2007.

522   Chemical and physical characteristics of nascent aerosol produced by bursting bubbles at a

523   model air-sea interface. *J. Geophys. Res.*, **112**, D21202, doi:10.1029/2007/JD008464.

524 König-Langlo, G., King, J.C., Pettré, P. 1998. Climatology of the three coastal Antarctic

525   stations Dumont d'Urville, Neumayer and Halley. *J. Geophys. Res.* **103**(D9), 10 935-10

526   946.

527 Kottmeier, C. and Fay, B. 1998. Trajectories in the Antarctic lower troposphere. *J. Geophys.*

528   *Res.* **103,** 10 947-10 959.

529 Krinner, G. and Genthon, C. 2003. Tropospheric transport of continental tracers towards

530   Antarctica under varying climatic conditions. *Tellus* **55B**, 54-70.

531 Lindberg, S.E. and Harris, R.C. 1983. Water and acid soluble trace metals in atmospheric

532   particles. *J. Geophys. Res.* **88**(C9), 5091-5100.

533   Marion, G.M. and Farren, R.E. 1999. Mineral solubilities in the Na-K-Mg-Ca-Cl-SO$_4$-H$_2$O

534   system: A re-evaluation of the sulfate chemistry in the Spencer-Møller-Weare model. *Geo-*

535   *chim. Cosmochim. Acta,* **63**, No. 9, 1305-1318.

536   Minikin, A., Legrand, M., Hall, J., Wagenbach, D., Kleefeld, C., Wolff, E., Pasteur, E.C., and

537   Ducroz, F. 1998. Sulfur-containing species (sulfate and methanesulfonate) in coastal Ant-

538   arctic aerosol and precipitation. *J. Geophys. Res*. **103**(D9), 10,975-10,990.

539   Monahan, E.C., Spiel, D.E., and Davidson, K.L. 1986. A model of marine aerosol generation

540   via whitecaps and wave disruption. In: *Oceanic Whitecaps* (edited by E. Monahan and

541   G.M. Niocaill). D. Reidel, Norwell, Mass., 167-174.

542   Mosher, B.W. 1986. The atmospheric biochemistry of selenium, PhD-Thesis. University of

543   Rhode Island, Kingston.

544   Mosher, B.W. and Duce, R.A. 1987. A global atmospheric selenium budget. *J. Geophys. Res.*

545   **92**(D11), 13,289-13,298.

546   Mosher, B.W., Duce, R.A., Prospero, J.M., Savoie, D.L. 1987. Atmospheric selenium: geo-

547   graphical distribution and ocean to atmosphere flux in the Pacific. *J. Geophys. Res.*

548   **92**(D11), 13,277-13,287.

549   Petit, J.R., Jouzel, J., Raynaud, D., Barkov, N.I., Barnola, J.-M., and co-authors. 1999. Cli-

550   mate and atmospheric history of the past 420,000 years from the Vostok ice core, Antarc-

551   tica. *Nature* **399***,* 429-436.

552   Piel, C. 2004. Variabilität physikalischer und chemischer Parameter des Aerosols in der ant-

553   arktischen Troposphäre. In: *Reports on Polar and Marine Research* **476** (ed. F. Riemann).

554   Alfred-Wegener-Inst. for Polar and Marine Res., Bremerhaven.

555   Planchon, F.A.M., Boutron, C.F., Barbante, C., Cozzi, G., Gaspari, V., Wolff, E.W., Ferrari,

556   C.P., and Cescon, P. 2002. Changes in heavy metals in Antarctic snow from Coats Land

557   since the mid-19th to the late-20th century. *Earth Planet. Sci. Lett.* **200**, 207-222.

Version 30.04.2008

558   Rankin, A.M., Auld, V., and Wolff, E.W. 2000. Frost flowers as a source of fractionated sea

559   salt aerosol in the polar regions. *Geophys. Res. Lett.* **27**(21), 3469-3472.

560   Rankin, A.M., Wolff, E.W., and Martin, S. 2002. Frost flowers: Implications for tropospheric

561   chemistry   and   ice   core   interpretation.   *J.   Geophys.   Res*.   **107**(D23),   4683,

562   doi:10.10129/2002JD002492.

563   Reinhardt, H., Kriews, M., Miller, H., Lüdke, C., Hoffmann, E., and Skole, J. 2003. Applica-

564   tion of LA-ICP-MS in polar ice core studies. Anal. Bioanal. Chem. 375, 1265-1275,

565   doi:10.1007/s00216-003-1793-5.

566   Ruth, U., Bigler, M., Röthlisberger, R., Siggaard-Andersen, M.-L., Kipfstuhl, S., and co-

567   authors. 2007. Ice core evidence for a very tight link between North Atlantic and east

568   Asian glacial climate. *Geophys. Res. Lett.* **34** L03706, doi:10.1029/2006GL02786.

569   Smith, J., Vance, D., Kemp, R.A, Archer, C., Toms, P., King, M., Zárate, M. 2003. Isotopic

570   constraints on the source of Argentinean loess – with implications for atmospheric circula-

571   tion and the provenance of Antarctic dust during recent glacial maxima. *Earth Planet. Sci.*

572   *Lett.* **212**, 181-196.

573   Tuncel, G., Aras, N.K., and Zoller, W.H. 1989. Temporal variations and sources of elements

574   in the South Pole Aatmosphere, 1. Nonenriched and moderately enriched elements. *J.*

575   *Geophys. Res.* **94**(D10), 13,025-13,038.

576   Turner, S.M., Harvey, M.J., Law, C.S., Nightingale, P.D., and Liss, P.S. 2004. Iron-induced

577   changes   in   oceanic   sulfur   biogeochemistry.   *Geophys.   Res.   Lett.*   **31**,   L14307,

578   doi:10.1029/2004GL020296.

579   Wagenbach, D. 1996. Coastal Antarctica: Atmospheric chemical composition and atmos-

580   pheric transport. In: *Chemical Exchange between the Atmosphere and polar snow* (ed.

581   E.W. Wolff and R.C. Bales). NATO ASI Series vol. **43***,* Springer-Verlag Berlin Heidel-

582   berg, 173-199.

Version 30.04.2008

583   Wagenbach, D., Görlach, U., Moser, K., and Münnich, K.O. 1988. Coastal Antarctic aerosol:

584   the seasonal pattern of its chemical composition and radionuclide content. *Tellus* **40B**, 426-

585   436.

586   Wagenbach, D., Ducroz, F., Mulvaney, R., Keck, L., Minikin, A., Legrand, M., Hall, J.S., and

587   Wolff, E.W. 1998. Sea salt aerosol in coastal Antarctic regions. *J. Geophys. Res.* **103**(D9),

588   10 961-10 974.

589   Wedepohl, K.H. 1995. The composition of the continental crust. *Geochim. Cosmochim. Acta*

590   **59**(7), 1217-1232.

591   Wen, H. and Carignan, J. 2007. Reviews on atmospheric selenium: Emission, speciation and

592   fate. *Atmos. Environ.* **41**, 7151-7165.

593   Wolff, E.W., and Suttie E.D. 1994. Antarctic snow record of southern hemisphere lead pollu-

594   tion. *Geophys. Res. Lett.* **21**(9), 781-784.

595   Wolff, E.W., Suttie, E.D., Peel, D.A. 1999. Antarctic snow record of cadmium, copper, and

596   zinc content during the twentieth century. *Atmos. Environ.* **33**, 1535-1541.

597   Wolff, E.W., Rankin, A.M., and Röthlisberger, R. 2003. An ice core indicator of Antarctic sea

598   ice production. *Geophys. Res. Lett.* **30**(22), 2158, doi:10.1029/2003GL018454.

599   Wolff, E.W., Fischer, H., Fundel, F., Ruth, U., Twarloh, B., and co-authors. 2006. Southern

600   Ocean sea-ice extent, productivity and iron flux over the past eight glacial cycles. *Nature*

601   **440**, 491-496, doi:10.1038/nature04614.

602   Wyputta, U. (1997). On the transport of trace elements into Antarctica using measurements at

603   the Georg-von-Neumayer station. *Tellus* **49B**, 93-111.

604   Zoller, W.H., Gladney, E.S., and Duce, R.A. 1974. Atmospheric concentration of trace metals

605   at the South Pole. *Science* **183**, 198-200.

Version 30.04.2008

606

607 *Table 1.* Instrumental ICP-QMS detection limits (IDL, n=60) and overall method detection

608 limits (MDL, n=49) corresponding to a typical, total sampling volume of 2.0×10^4 m^3. (MDL

609 for IC-analysis given in parenthesis)

610

element	IDL	MDL
Li[pg m^{-3}]	0.12	0.21
Na[pg m^{-3}]	16	1800 (300)
Mg[pg m^{-3}]	0.44	300 (170)
K[pg m^{-3}]	32	330 (100)
Ca[pg m^{-3}]	5.0	1300 (140)
Sr[pg m^{-3}]	0.02	12
Al[pg m^{-3}]	10	220
La[pg m^{-3}]	0.005	0.07
Ce[pg m^{-3}]	0.002	0.17
Nd[pg m^{-3}]	0.006	0.09
Se[pg m^{-3}]	2.7	3.1

611

612

613

614 *Table 2.* Inter-comparison of trace elements measured by IC versus ICP-QMS: Results refer

615 to a reduced major axis regression (RMA) with slope = m, y-axis intercept = b, regression

616 coefficient = r^2.

617

Element	m	b [ng m^{-3}]	r^2
Na	1.00±0.05	24± 35	0.52
K	0.76±0.04	-0.71±1.4	0.43
Mg	1.14±0.07	-5.94±6.5	0.35
Ca	1.51±0.09	-2.05±2.1	0.42

618

Version 30.04.2008

619

620 *Table 3*. Summary of trace element composition of the aerosol measured during five years

621 (March 1999 through December 2003) at Neumayer Station via ICP-QMS, except for Ca and

622 K which were taken from IC-analysis. Atmospheric mean concentrations (±std) refer to stan-

623 dard pressure (1013 hPa) and 273.16 K.

624

element	overall mean	winter Apr. to Oct.	winter range	summer Nov. to Mar.	summer range
Li[pg m^{-3}]	6.1±4.1	6.9±4.5	0.2–26.5	4.9±3.1	0.17–15.0
Na[ng m^{-3}]	330±340	400±400	41-3860	220±160	0.3-820
Mg[ng m^{-3}]	52±66	62±80	6.8-760	31±22	0.17-10
K[ng m^{-3}]	16±15	17±13	0.1*-6.1	14±17	0.1*-12
Ca[ng m^{-3}]	15±15	19±17	0.14*-67	11±8.6	0.14*-26.4
Al[ng m^{-3}]	1.0±0.7	0.84±0.6	0.22*-3.2	1.3±0.7	0.23-3.7
Sr[ng m^{-3}]	0.29±0.27	0.36±0.31	0.012*-2.6	0.19±0.13	0.012*-0.53
La[pg m^{-3}]	0.86±0.7	0.56±0.5	0.07*-3.1	1.32±0.8	0.07*-5.8
Ce[pg m^{-3}]	1.6±1.3	1.0±0.8	0.17*-5.5	2.5±1. 5	0.17*-10.5
Nd[pg m^{-3}]	0.7±0.6	0.47±0.45	0.09*-2.7	1.1±0.6	0.09*-4.4
Se[pg m^{-3}]	19±18	16±11	3.1*-82	25±24	3.1*-160

625   *   method detection limit (MDL)
626

627

628 *Table 4.* Al, La, Na, and Se concentrations (±std) measured in Antarctic aerosol samples.

629

element	winter	summer	sampling period	site[a]
Al	-	570±170	10/1970	SP (Zoller et al., 1974)
[pg m^{-3}]	300±40	830±410	1971/75/76/78	SP (Cunningham & Zoller, 1981)
	320±110	730±240	2/1979 – 11/1983	SP (Tuncel et al., 1989)
	-	194±19	12/1984 – 02/1985	AP (Dick, 1991)
	9470[b]	13290[b]	1985-1988	AP (Artaxo et al., 1992)
	840±600	1270±700	3/1999 – 12/2003	NM, this study
La	-	0.51±0.37	10/1970	SP (Zoller et al., 1974)
[pg m^{-3}]	< 2	0.78±0.25	1971/75/76/78	SP (Cunningham & Zoller, 1981)
	0.43±0.11	0.56±0.21	2/1979 – 11/1983	SP (Tuncel et al., 1989)
	0.56±0.5	1.32±0.8	3/1999 – 12/2003	NM, this study
Na	-	7.2±3.8	10/1970	SP (Zoller et al., 1974)
[ng m^{-3}]	40±31	5.1±1.7	1971/75/76/78	SP (Cunningham & Zoller, 1981)
	31±14	8.7±3.2	2/1979 – 11/1983	SP (Tuncel et al., 1989)
	869.9[b]	1046.2[b]	1985-1988	AP (Artaxo et al., 1992)
	-	27.6±0.4	12/1984 – 02/1985	AP (Dick, 1991)
	400±400	220±160	3/1999 – 12/2003	NM, this study
Se	-	5.6±1.2	10/1970	SP (Zoller et al., 1974)
[pg m^{-3}]	6.9±2.7	6.3±6	1971/75/76/78	SP (Cunningham & Zoller, 1981)
	4.8±0.8	8.4±1.6	2/1979 – 11/1983	SP (Tuncel et al., 1989)
	118[b]	122[b]	1/1983 – 12/1984	AP (Artaxo et al., 1992)
	16±11	25±24	3/1999 – 12/2003	NM, this study

630 [a]AP = Antarctic Peninsula, SP = South Pole, NM = Neumayer
631 [b]sum of fine and coarse mode
632

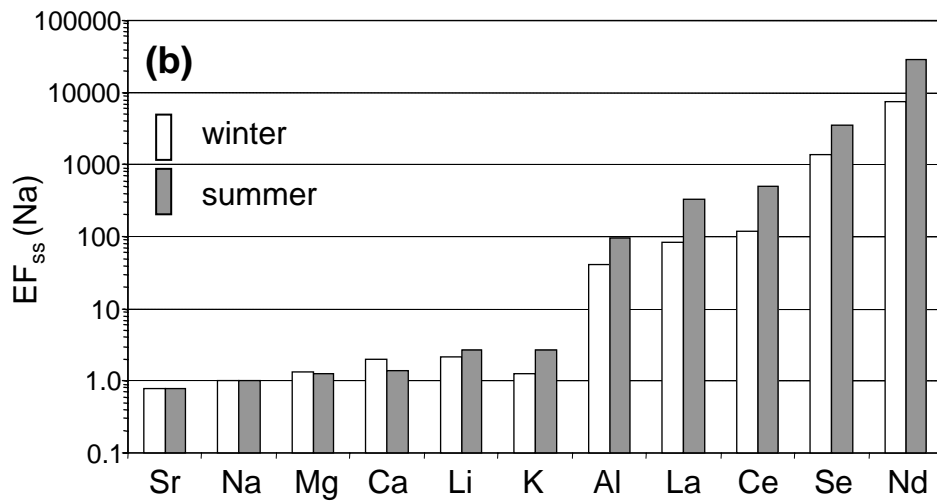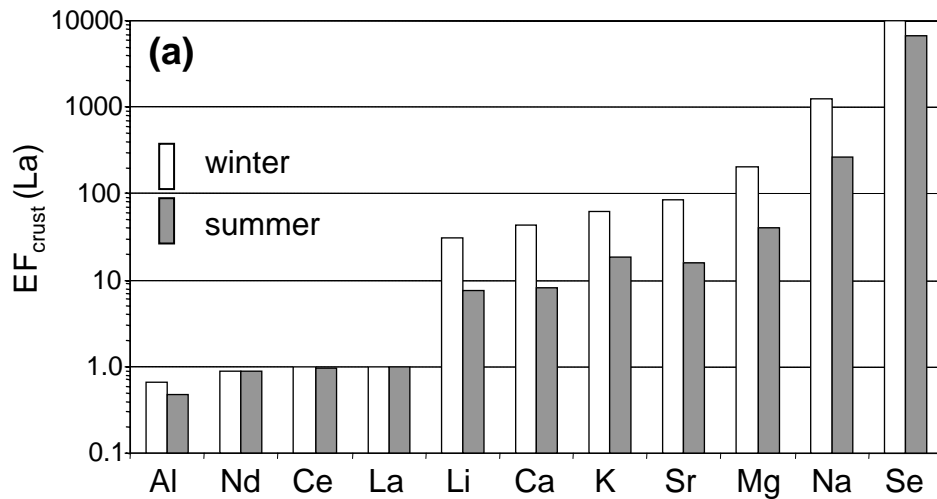Version 30.04.2008

633   **FIGURES**
634
635
636   *Fig. 1:* (a) Mean element enrichment factors with respect to earth crust (EF_{crust}) and (b) sea

637   salt composition (EF_{ss}) of Neumayer aerosol samples dissected for summer (November

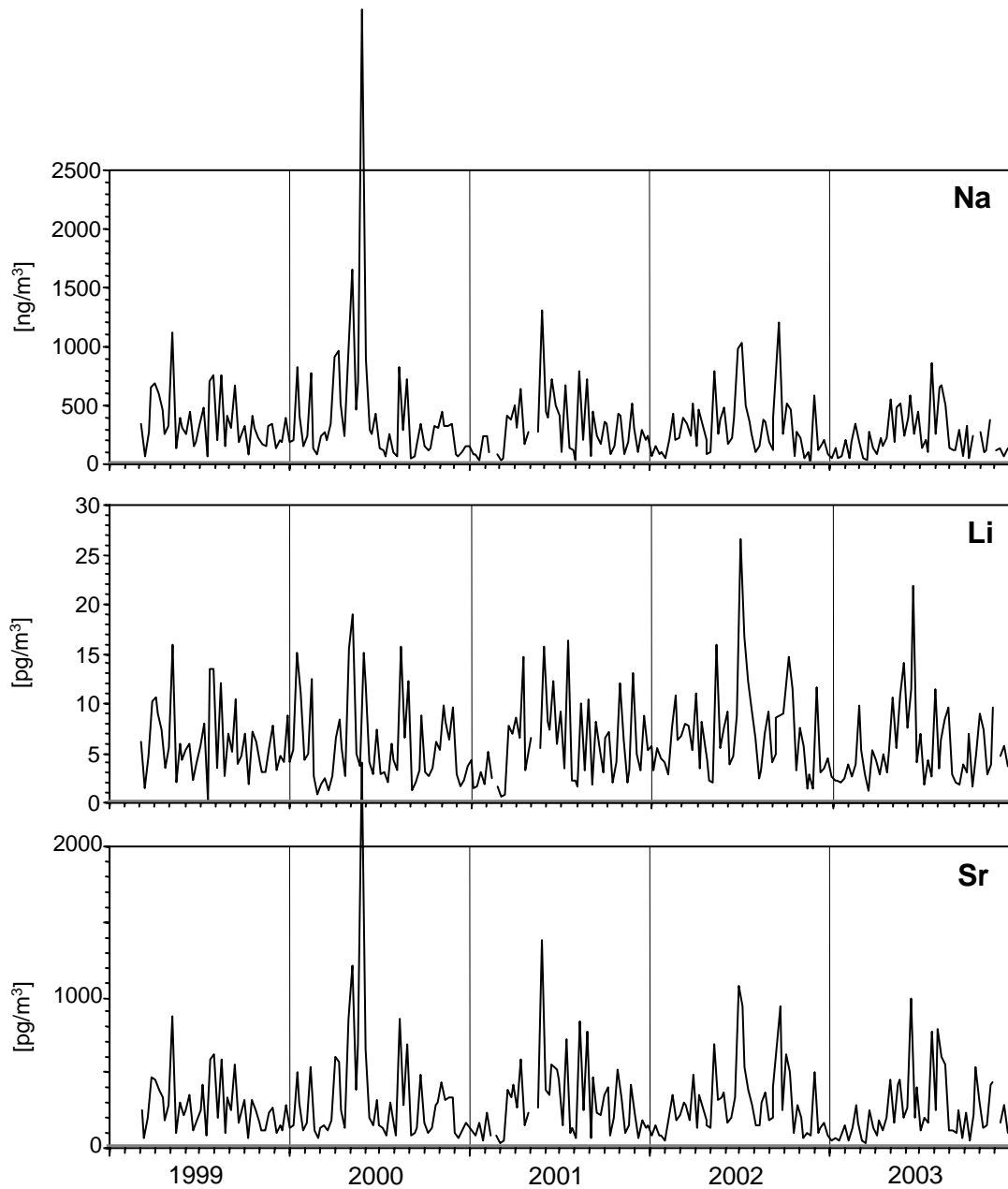638   through March) and winter (April through October), respectively.

639

640   *Fig. 2:* Atmospheric Na, Li, and Sr concentrations measured at Neumayer Station at weekly

641   time resolution. The grey bars mark the method detection limits.

642

643   *Fig. 3:* Same as Figure 2 but for Al, La, Ce, and Nd.

644

645   *Fig. 4:* Pie diagram of the aerosol composition (weight percent referring to the sum of the

646   measured species) at Neumayer during winter and summer, respectively.

647

648   *Fig. 5:* Mean annual cycle of major mass fractions in Neumayer aerosol samples: Sea salt

649   (circles), biogenic sulfur (i.e. the sum of MS and nss-SO_4^{2-}, drawn line), and mineral dust

650   (diamonds) portion.

651

652   *Fig. 6:* Seasonality of monthly concentration mean of sea salt (Na) and mineral dust (La)

653   reference elements. Values correspond to 5 years of observation (i.e. about 20 samples per

654   month). Error bars indicate the respective standard deviation.

655

656   *Fig. 7:* Time series of wind velocity at Neumayer during the sampling period displayed in the

657   same temporal resolution as filter sampling (seven days, thin line), and 6 points moving aver-

658   age (bold grey line).

Version 30.04.2008

659

660 *Fig. 8:* Notched box plots for enrichment factors respecting standard mean ocean water com-

661 position for the sea salt portion of Li, K, Mg, Ca, and Sr. Lines in the middle of the boxes

662 represent sample medians (values are given aside), lower and upper lines of the boxes are the

663 25th and 75th percentiles, whiskers show the range of the sample values while outliers are

664 marked by "+" signs. The widths of the notches indicate the confidence interval of the me-

665 dian.

666

667 *Fig. 9:* Double-logarithmic plot of ssLi, ssMg, and ssSr vs. ssNa. Bold grey lines represent

668 the relation for standard mean ocean water.

669

670 *Fig. 10:* Time series of Se and MS (shifted y-axis) concentrations measured at Neumayer.

671 The grey bar marks the method detection limit for Se.

672

Figure 1: (a) Mean element enrichment factors with respect to earth crust (EF_{crust}) and (b) sea salt composition (EF_{ss}) of Neumayer aerosol samples dissected for summer (November through March) and winter (April through October), respectively.

Figure 2: Atmospheric Na, Li, and Sr concentrations measured at Neumayer Station at weekly time resolution. The grey bars mark the method detection limits.
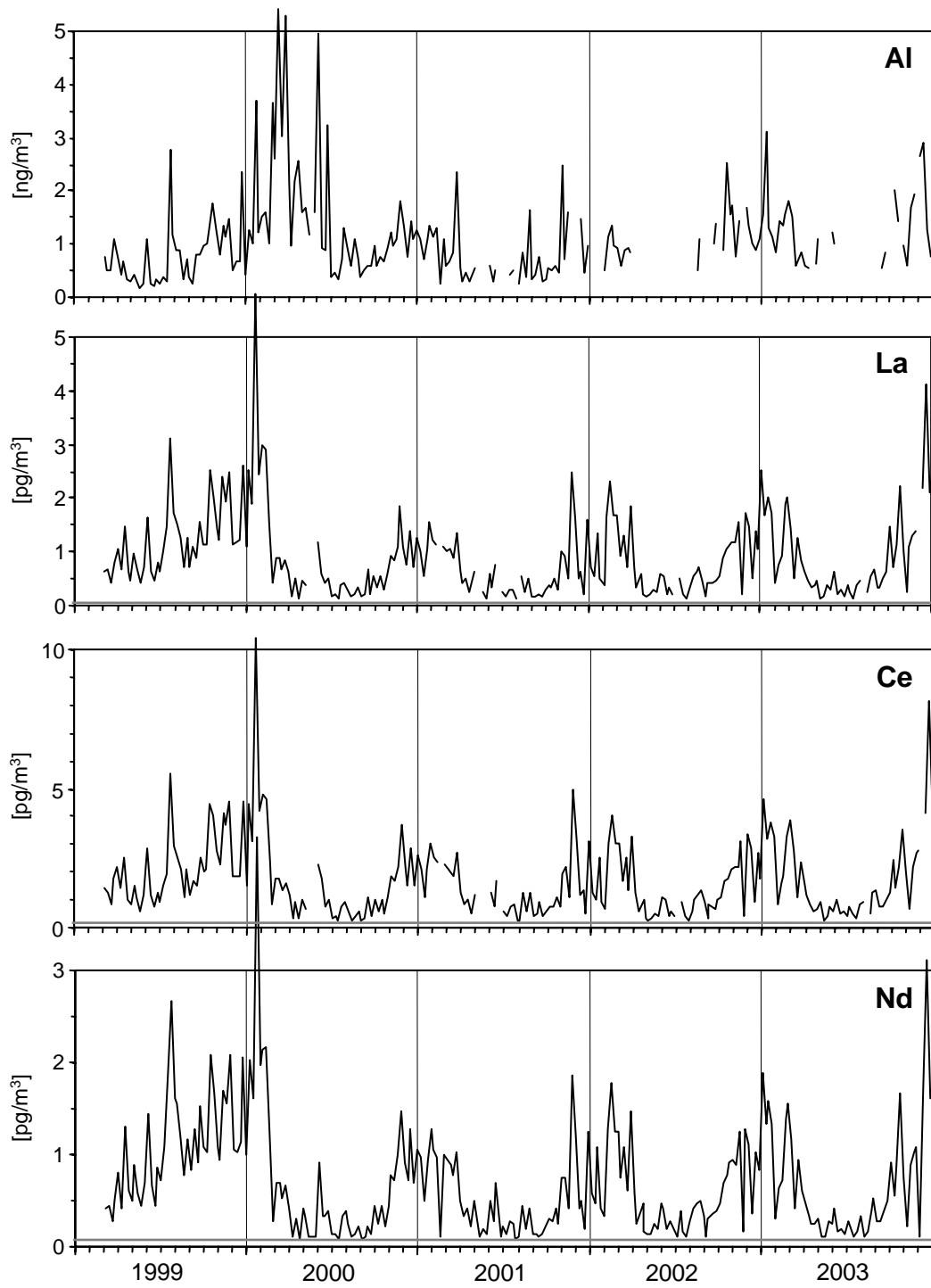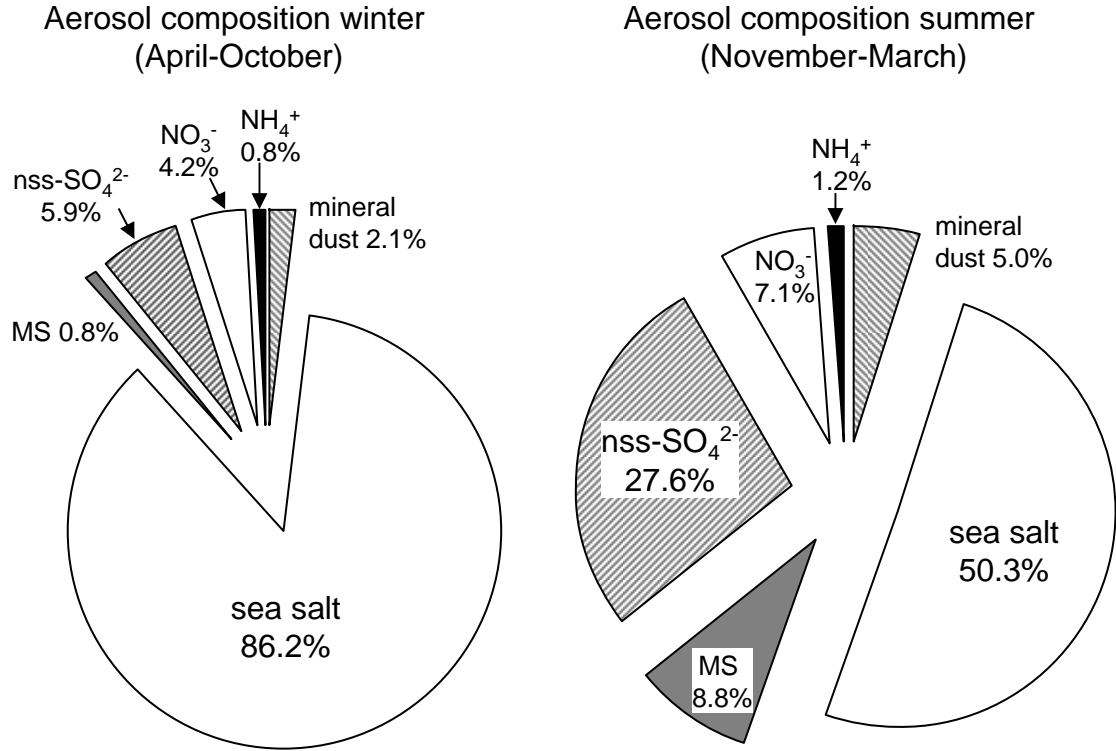
Figure 3: Same as Figure 2 but for Al, La, Ce, and Nd.

Figure 4: Pie diagram of the aerosol composition (weight percent referring to the sum of the measured species) at Neumayer during winter and summer, respectively.
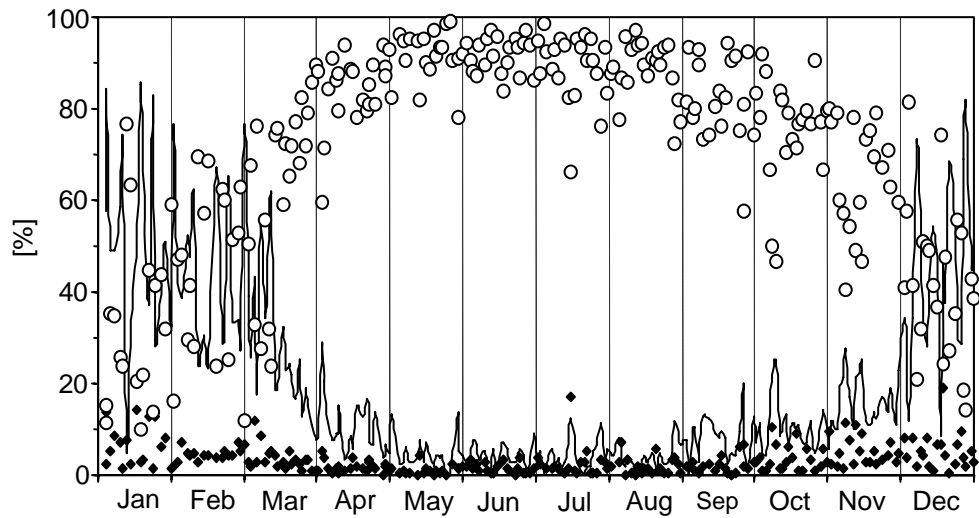
Figure 5: Mean annual cycle of major mass fractions in Neumayer aerosol samples: Sea salt (circles), biogenic sulfur (i.e. the sum of MS and nss-SO_4^{2-}, drawn line), and mineral dust (diamonds) portion.
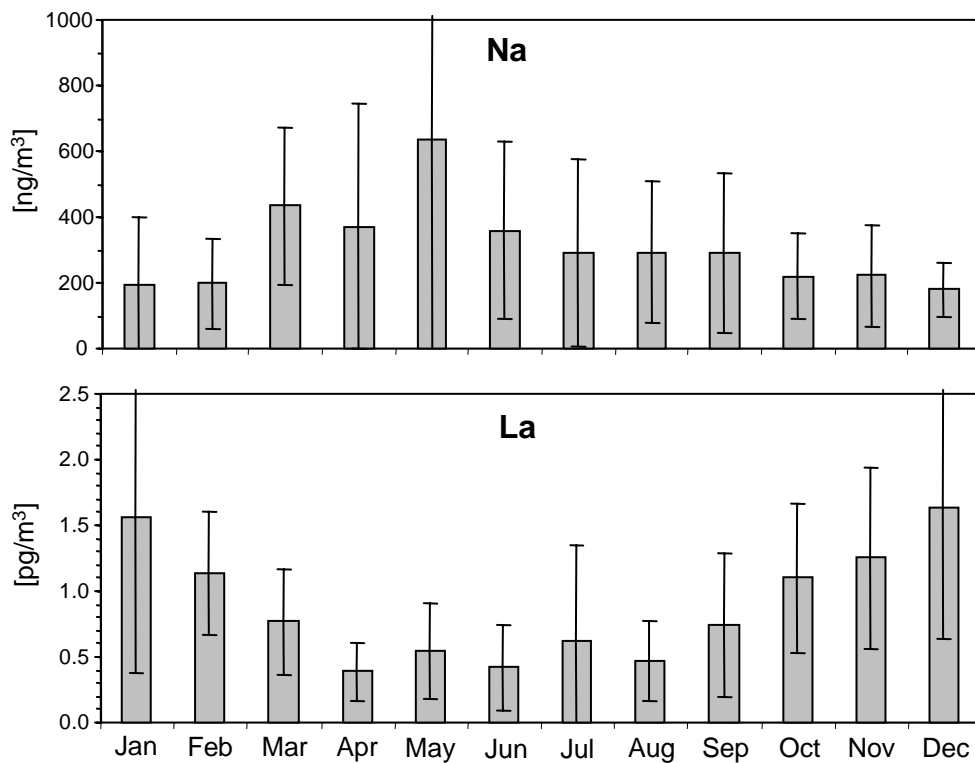
Figure 6: Seasonality of monthly concentration means of sea salt (Na) and mineral dust (La) reference elements. Values correspond to 5 years of observation (i.e. about 20 samples per month). Error bars indicate the respective standard deviation.
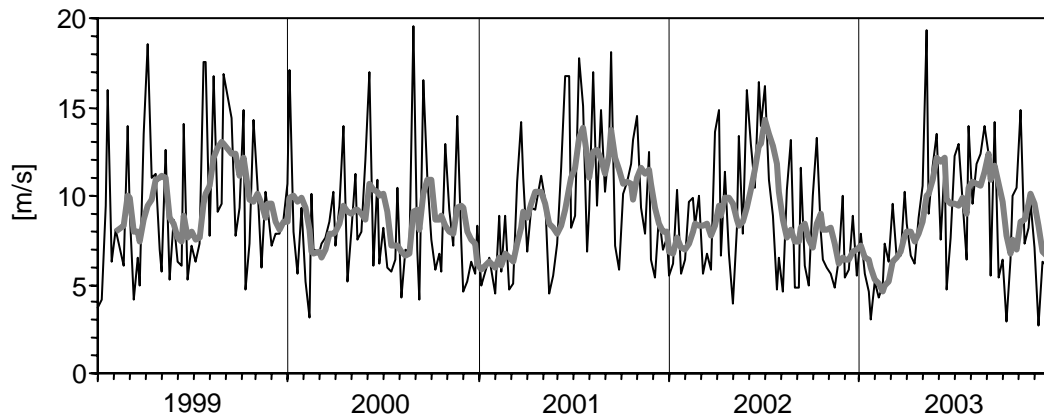
Figure 7: Time series of wind velocity at Neumayer during the sampling period displayed in the same temporal resolution as filter sampling (seven days, thin line), and 6 points moving average (bold grey line).
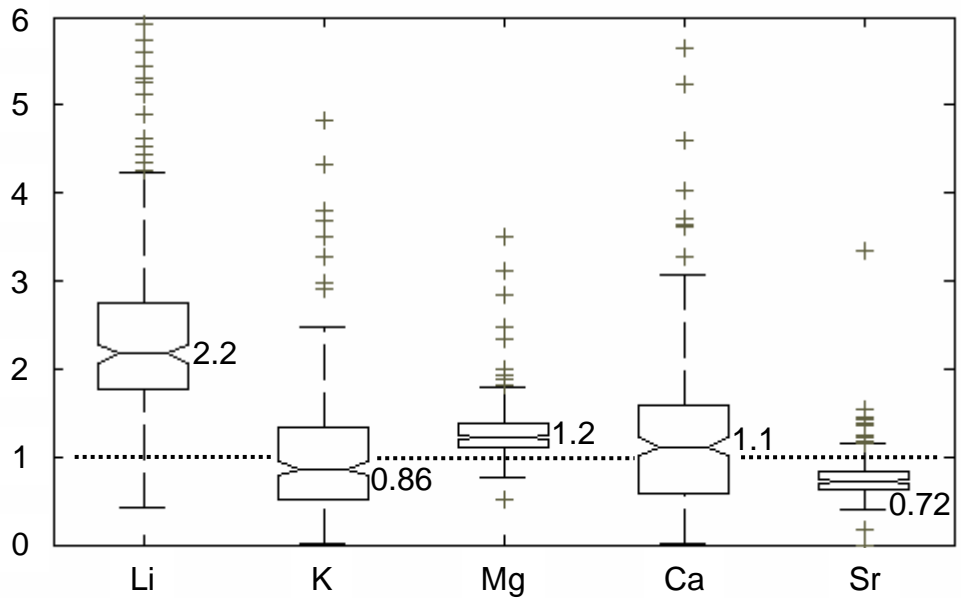
Figure 8: Notched box plots for enrichment factors respecting standard mean ocean water composition for the sea salt portion of Li, K, Mg, Ca, and Sr. Lines in the middle of the boxes represent sample medians (values are given aside), lower and upper lines of the boxes are the 25th and 75th percentiles, whiskers show the range of the sample values while outliers are marked by "+" signs. The widths of the notches indicate the confidence interval of the median.
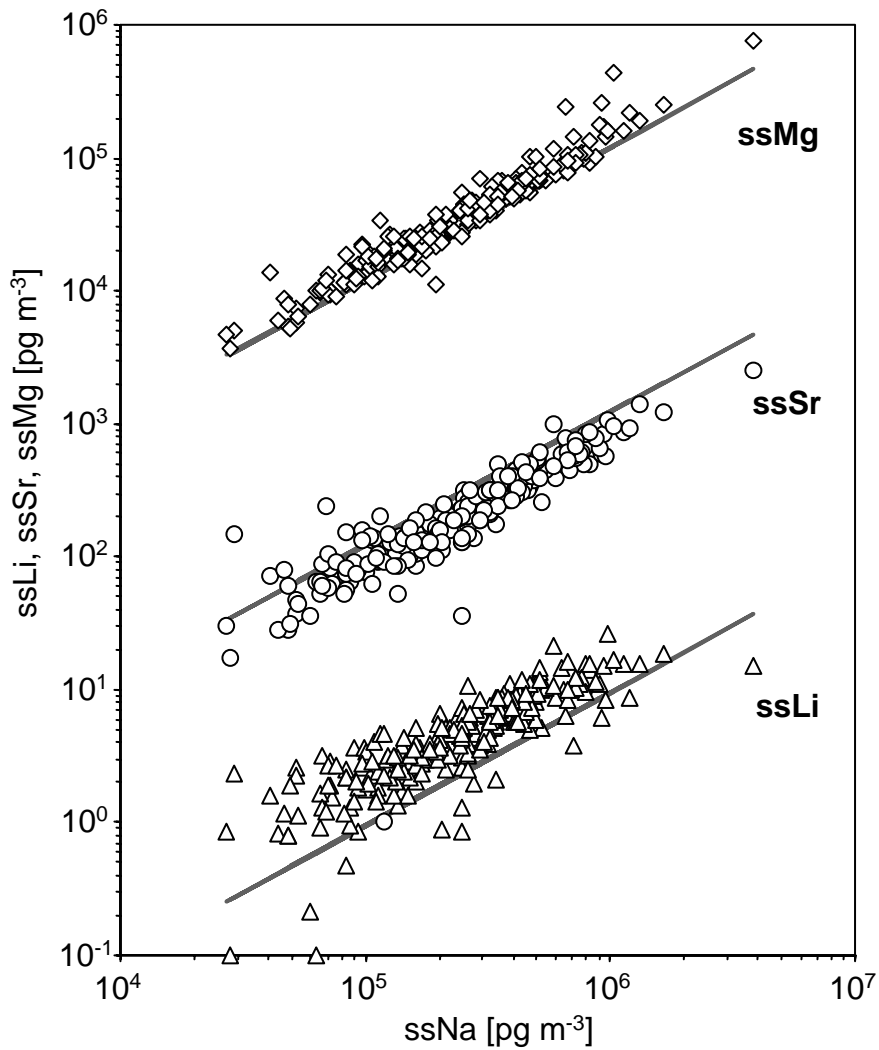
Figure 9: Double-logarithmic plot of ssLi, ssMg, and ssSr vs. ssNa. Bold grey lines represent the relation for standard mean ocean water.

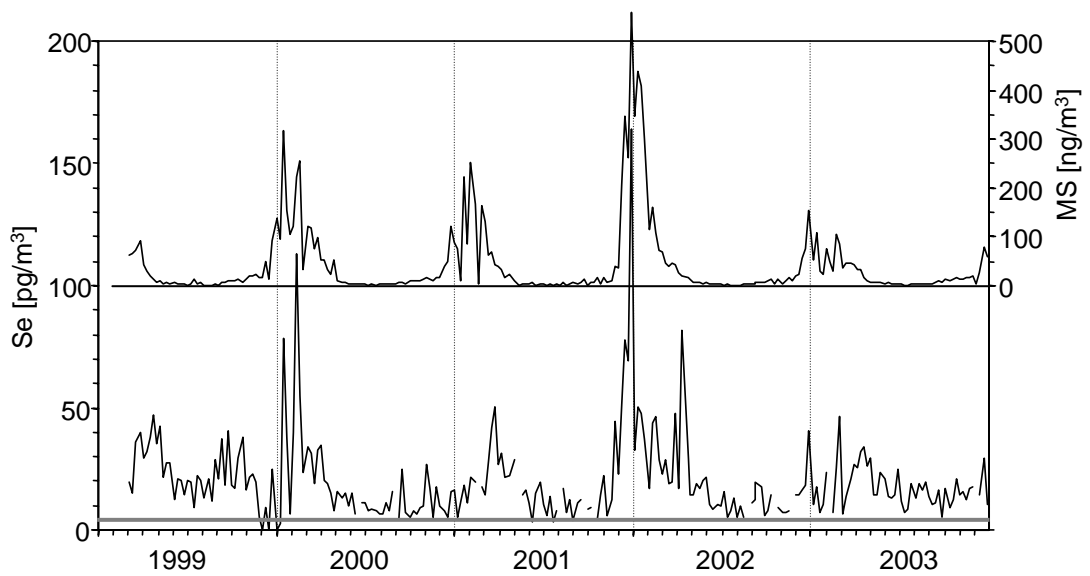**Figure 10:** Time series of Se and MS (shifted y-axis) concentrations measured at Neumayer. The grey bar marks the MDL for Se.